ROYAL SOCIETY OF CHEMISTRY

Check for updates

Sprayable copper and copper–zinc nanowires inks for antiviral surface coating

Chaochao Pan, [ID] [a] Kruttika S. Phadke, [b] Zheng Li, [ID] [c] Gaoyuan Ouyang, [d] Tae-hoon Kim, [d] Lin Zhou, [ID] [d] Julie Slaughter, [d] Bryan Bellaire, [b] Shenqiang Ren [ID] [c] and Jun Cui [ID] ★[ad]

Copper alloys are known for their high antimicrobial efficacy. Retrofitting high-touch surfaces in public space with solid copper components is expensive and often impractical. Directly coating copper onto these high-touch surfaces can be achieved with hot or cold spray, but the procedure is complicated and requires special equipment. This article reports on the development of sprayable copper and copper–zinc nanowire inks for antiviral surface coating applications. Our results show that copper nanowires inactivate the SARS-CoV-2 virus faster than bulk copper. And a trace amount of zinc addition has a significant effect in enhancing the virucidal effect. More importantly, these nanowire inks are sprayable. They can be easily applied on high-touch surfaces with a spray can. When combined with common chemical disinfectants, the copper-based nanowire ink spray may prolong the disinfecting effect well after application.

1. Introduction

The severe acute respiratory syndrome coronavirus 2 (SARS-CoV-2) has infected more than 418 million people and caused over 5 million deaths worldwide as of February 2022.[1] While vaccines have been available since February 2021, vaccinating a critical percentage of the population to achieve herd immunity takes time and resources. And the virus mutation undermines vaccine efficacy.[2] The best practice is to avoid contact with the virus in the first place. Besides inhalation of fine respiratory droplets carrying the infectious virus, people can be infected by touching mouth, nose, or eye with hands that have been contaminated by touching virus contaminated surfaces.[3] Studies have shown that SARS-CoV-2 can survive on inorganic surfaces for hours to days, depending on the surface material and environmental conditions. Doremalen *et al.*[4] found that at 40% relative humidity and 21–23 °C, the median half-life of the viable virus is 0.8 h after being deposited on a copper surface, 5.6 h on a stainless-steel surface, and 6.8 h on a plastic surface. Riddell *et al.*[5] isolated viable SARS-CoV-2 virus from common surfaces such as glass, stainless steel, paper, and polymer banknotes 28 d after the initial virus inoculation under ambient

conditions, but they did not study copper surfaces. Warnes *et al.*[6] found that copper and brass inactivated the virus in less than 60 min, with the deactivation rate proportional to the percentage of copper. On non-copper-containing surfaces, the virus retained infectivity after five days.

Compared with other surfaces, copper and copper alloys show outstanding virucidal effects. Copper has been proven effective in inactivating not only viruses but also bacteria, fungi, and yeasts when they are in contact.[7–9] The exact mechanism is not yet confirmed. But in general, it was agreed that the virucidal effect is the result of the released copper ions attacking the cell membrane[7,10] and virus RNA.[11] The antimicrobial effect of copper was recognized by ancient human civilizations as early as 2400 B.C. As recorded in an ancient medical text Smith Papyrus, copper was used to sterilizing wounds and drinking water.[8] Since then, copper had found various medical applications until it became obsolete when antibiotics became commercially available in the 1930s.[7] The global spread of antibiotic-resistant bacteria drew intensive attention to copper again for its antimicrobial effect and the potential application as a self-disinfecting material in the hospital environment where the risk of infection by the bacteria on a non-sterilized surface is high.[12] Several hospital trials of using copper as the material for high-touch surfaces have been conducted, and the results are encouraging. A 10 weeks trial conducted in Selly Oak Hospital, Birmingham, UK[13] showed that the copper-containing toilet seat, tap handles, and door push plate had between 90% to 100% fewer median numbers of microorganisms than their non-copper-containing counterparts in the same ward. In a study carried out in Highpoint Health hospital, Indiana, USA,

aDepartment of Materials Science & Engineering, Iowa State University, Ames, IA 50011, USA

bDepartment of Veterinary Microbiology & Preventive Medicine, Iowa State University, Ames, IA 50011, USA

cDepartment of Mechanical and Aerospace Engineering, University at Buffalo, Buffalo, NY 14260, USA

dDivision of Materials Science & Engineering, Ames Laboratory, Ames, IA, 50011, USA. E-mail: cuijun@iastate.edu

intensive care unit beds were encapsulated with U.S. EPA-registered antimicrobial copper materials and the bacteria concentration of high-touch surfaces was monitored and compared with that of traditional beds with plastic surfaces.[12] During the 11 months of patients' stay, the bacteria on surfaces of copper encapsulated beds was reduced by 94%, and the microbial burden was maintained below the terminal cleaning and disinfection risk threshold. In all these studies, routine daily and terminal cleaning regimes are followed for both copper fittings and the control fittings.

Despite the success in these trials, stainless steel is still the most widely used metal in healthcare facilities. Replacing all stainless-steel parts is expensive and often not practical. Furthermore, copper surfaces need regular cleaning to remove the build-ups in order to be in direct contact with the virus. A convenient method that allows cost-effective deployment of the fresh copper surface may lower the barrier to adopting copper as the standard surface material for healthcare facilities, public transportation systems, offices, and restaurants. Here, we report our work on developing a sprayable ink containing copper nanowires (CuNWs) and copper–zinc nanowires (CuZnNWs), which can be conveniently sprayed on hygiene-sensitive surfaces forming an antimicrobial coating.

2. Experimental methods

2.1. Ink preparation and coating

The precursor solution for the pure copper nanowires was prepared by mixing 2.4 g of copper chloride, 14.55 g of hexadecylamine (90%, TCI), 3.9 g of glucose (99.5%, VWR Chemicals) in 900 mL of DI Water in a glass bottle. This solution was magnetically stirred for 12 h, resulting in a uniformly mixed, homogenous feedstock solution. For copper–zinc precursor, an additional 0.6146 g of zinc acetate dihydrate was added. The feedstock solutions were heated in a hydrothermal reactor at 100 °C for 12 h. After the culmination of the reaction, the solution was centrifuged with 5000 rpm for 10 min, and the precipitate was collected. The water-soluble copper slurry was formed because of sedimentation. The product was washed three times by centrifuging and re-dispersing in DI water. Finally, the ink for coating was achieved by diluting the slurry into 3.3 wt% water solution, then sonicated for 15 min followed by filtering with 180 μm sieve. A pure copper plate of 0.5 mm thickness (99.99% McMaster-Carr) was used as substrate material for the coating. The copper plate was punched into 5 mm diameter disks, polished with 600 grit sandpaper, and cleaned with acetone. The disks were covered with 40 μL ink, then dried in air, which left a uniform coating on the disk.

2.2. Coating composition

Composition analysis was carried out at the Analytical Chemistry Services of the Iowa State University Veterinary Diagnostic Laboratory. Samples were analysed for copper and zinc content using an Inductively Coupled Plasma Mass Spectrometry (Plasma Quant MS Elite, Analytik Jena Inc. Woburn, MA, USA) in CRI mode with hydrogen as the skimmer gas. Standards were obtained from Inorganic Ventures (Christiansburg, VA). 15 mL centrifuge tubes and trace mineral grade nitric acid were purchased from Fisher Scientific (Pittsburgh, PA). Samples were partitioned into 15 mL tubes and digested in 70% nitric acid at 70 °C in a dry heat bath for 2 h. After digestion, samples were diluted using 1% nitric acid. Samples with elevated copper content occasionally needed an additional dilution made using 1% nitric acid and were analysed by ICP-MS after the dilution. For copper and zinc analysis, yttrium was used as internal standards for the ICP-MS analysis.

2.3. Coating crystal structure and morphology

X-ray diffraction patterns of CuNW and CuZnNW were collected from air-dried inks using a Panalytical X'Pert X-ray diffractometer equipped with copper source and operated at 40 kV and 45 mA. The morphology of CuNW and CuZnNW coatings is characterized in an FEI Inspect F50 field emission gun SEM using a secondary electron detector.

2.4. Electrochemical testing

An aqueous solution of calcium chloride ($CaCl_2$) with 15% (w/v) concentration was prepared by dissolving 7.5 g of calcium chloride in 25 mL of deionized water and stirred in a vortex mixer for 5 min. The electrochemical measurements were conducted using an electrochemical workstation (CHI 600). For a typical three-electrode measurement, the printed copper film forms the working electrode. The AgCl electrode functions as the reference electrode, and the platinum electrode forms the opposite electrode.

2.5. Virus infection and viable cell detection

Confluent monolayers of VeroE6 cells (CRL-1586; ATCC) cultured in Dulbecco's Modified Eagle Medium (DMEM, Corning) containing 5% FBS at 37 °C under 5% CO_2. SARS CoV-2 (NR-52281) isolated from a COVID-19 patient in Washington, USA, was acquired from BEI. The virus was passaged up to 3 passages to get a titer of 1.4×10^7 PFU ml^{-1}. Vero E6 cells were plated out in a 96 well plate at a cell density of 2×10^4 cells per well and incubated at 37 °C under 5% CO_2 overnight. To test the antiviral properties of a material, 1×10^4 PFU of SARS CoV-2 in a 50 μL volume was treated with pure copper, CuNW, or Cu–ZnNW coupons. At 5, 10, 20, and 40 min, VeroE6 cells in a 96 well plate were infected with 10 μL or 2×10^3 PFU of treated virus. Cells were incubated at 37 °C under 5% CO_2 for 3 days. After 3 days, lactate dehydrogenase (LDH) activity in the cell culture medium was measured using CyQuant LDH Cytotoxicity assay kit (Invitrogen) as per the manufacturer's recommended protocol. 50 μL of cell culture medium was briefly mixed with 50 μL reaction buffer in a 96 well plate. The plate was incubated at room temperature for 30 min. After 30 min, 50 μL of Stop solution was added. Absorbance (A) was measured at 490 nm and 680 nm, and corrected absorbance was obtained by subtracting 680 nm absorbance from 490 nm absorbance. LDH value measured indicates the number of lysed cells present in the medium, which is correlated with the cytopathic effect (CPE) caused by viral infection. LDH activity in uninfected and

infected cells (with no treatment) was used as negative and positive controls, respectively. Antiviral activity of the materials was measured as: $[1 - (A_{\text{treated}} - A_{\text{uninfected}})] \times 100$.

2.6. Thermal gravimetric analysis

Thermal gravimetric analysis (TGA) was performed on the HDA without any nanowire inks and the dried CuNW powder with HDA residuals under nitrogen flow with 10 K min^{-1} heating rate, using thermogravimetric analyzer (SDT Q600).

3. Results and discussion

3.1. Morphology of the nanowires in the coatings

CuNWs and CuZnNW inks can be prepared with a simple procedure. These nanowire inks can be dip-coated or air-sprayed on plastic, glass, or stainless-steel surfaces, and dried at room temperature. Compared with the "cold" spraying method, where the nozzle temperature is about 500 °C,[14] the coating process of the developed nanowire inks doesn't require any heating. Once coated, these nanowires are tangled together, forming a network, and bonded to the substrate. The coating thickness is about 1.7 μm, as determined by surface profilometry (KLA-Tencor Alpha-Steop IQ). Fig. 1(a) and (d) show the scanning electron microscopy images of the CuNW and CuZnNW networks, respectively. One interesting feature of these networks is the embedded particles (∼200 nm). Composition analysis using energy-dispersive X-ray spectroscopy revealed that these particles have no noticeable chemical composition difference from the corresponding nanowires. These particles formed when the nuclei growth was isotropic during the synthesis instead of along the preferred direction. Both CuNW and CuZnNW nanowires are about 60 nm in diameter with a 2.2 nm thick oxide layer, as depicted by the high-angle annular dark-field (HAADF) scanning transmission electron microscopy (STEM) images in Fig. 1(b) and (e). Their length exceeds 10 μm. Further examination using STEM imaging revealed that both nanowires are crystalline, and there

is no obvious structural difference between CuNW and CuZnNW, as shown in Fig. 1(c) and (f).

Since these nanowires coatings are designed for high-touch surfaces, their ability to penetrate human's skin and trigger toxicological responses must be evaluated. Many efforts have been directed to understand the mechanism for particle penetration through the top layer of skin. Nanoparticle dimensions are considered the most important parameters because chemical penetration into the skin most commonly occurs through the lipidic matrix that fills a gap of 75 nm.[15] Honeywell-Nguyen et al. showed that 100–130 nm rigid particles can only reach the superficial layer of the stratum corneum.[16] However, Tinkle et al. showed that fluorescein isothiocyanate conjugated dextran beads as large as 0.5–1.0 μm could penetrate the stratum corneum and reach the epidermis layer when the skin was massaged with these particles.[17] They also showed that beads bigger than 2 μm could not penetrate the stratum corneum. Based on these studies, the concern on CuNW and CuZnNW penetrating human skin could be dismissed because their lengths are over 10 μm, and they are tangled. However, these 200 nm copper particles embedded in the nanowire network remain a concern. They could penetrate the top layer of skin when people forcefully touch the surface coated with these particles. These particles are the results of isotropic growth during nano-synthesis. They could be removed with an optimized synthesis condition or by a more rigorous washing procedure.

3.2. Compositions of CuNWs and CuZnNWs

The added Zn was expected to form either elemental pure zinc or copper–zinc alloy. In the first case, the X-ray diffraction pattern would show distinct zinc peaks, and in the second case, the copper diffraction peak will shift to lower angles due to the lattice parameter increase. However, neither of them was found in the X-ray diffraction patterns. The X-ray diffraction patterns of CuNW and CuZnNW are identical, indicating the amount of zinc inclusion is below the detection limit of the X-ray powder diffraction method. The composition analysis using inductively coupled plasma mass spectroscopy showed 0.16 at% zinc in the filtered CuZnNW ink.

3.3. Electrochemical testing

The process of copper and its alloy releasing copper ions to microorganisms is an oxidation reaction, which can be characterized by cyclic voltammetry, as shown in Fig. 2. The anodic peak of CuNW at about −0.64 V quickly faded away as the corrosion progresses, indicating the release of copper ions from CuNW is acute but unsustainable. In comparison, the pristine CuZnNW has an additional anodic peak at −0.27 V. This peak may correspond to the oxidation of elemental zinc. Unlike CuNW, CuZnNW remains highly reactive up to 30 min's corrosion. It appears that CuZnNW releases copper ions more steadily and sustainably compared to CuNW. This behavior is expected as a copper–zinc alloy (brass) is known to be more corrosion resistive than pure copper.
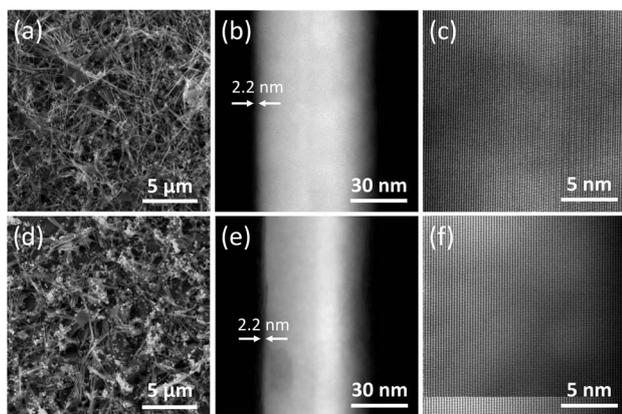

Fig. 1 Scanning electron microscopy images of (a) CuNW and (d) CuZnNW coating; HAADF STEM images of (b) CuNW and (e) CuZnNW; high-resolution HAADF STEM images of (c) CuNW and (f) CuZnNW taken under the [112] zone axis of Cu.
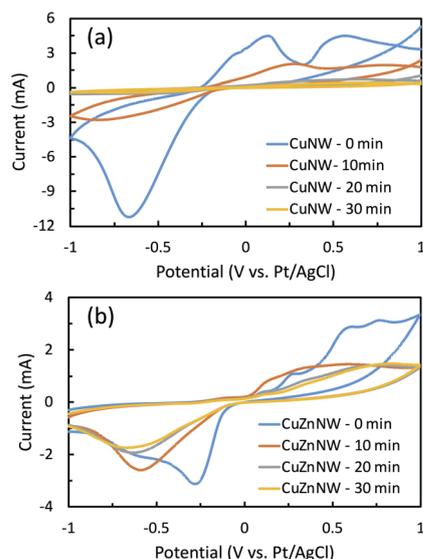
Fig. 2 Cyclic voltammetry curves of (a) CuNW and (b) CuZnNW. The reference electrode Ag–AgCl/saturated KCl was calibrated as 0.197 V.

3.4. Virucidal effect of the coatings

The virucidal effects of these nanowire coatings are evaluated by measuring the Vero E6 cell viability after incubation with the SARS CoV-2 virus that has been in contact with copper-based disks for up to 40 min. Cell viability is a measure of the proportion of live cells within a population. There are three types of copper-based disks used in the tests. The first type is made of pure copper with 5 mm diameter and 0.5 mm thickness. The second and the third types were the same as the first type, except that they are dip-coated with CuNW and CuZnNW inks, respectively.

To baseline the uninfected cases, the viability of Vero E6 cells incubated for 72 h at 37 °C and 5% CO_2 was measured. This reflects normal cell metabolic activity. It was normalized as 100% and plotted in Fig. 3 as dotted lines. To examine the effect of copper treatment on cell viability without virus, we incubated the three types of copper disks in phosphate buffered saline

(PBS) for 5, 10, 20, and 40 min, at 37 °C. Vero E6 cells were treated with 10 μL of this treated PBS and the viability was measured after 72 h of incubation. We found that after copper treatment, the percentages of live cells did not drop below the uninfected baseline, regardless of the types of the copper disks (Fig. 3(a)). This result proves no cytotoxicity of the bulk copper and copper nanowires.

To baseline the virus-infected cases, we incubated the Vero E6 cells with the SARS CoV-2 virus for 72 h. The cell viability is plotted as a dashed line in Fig. 3(b). This reflects the highest percentage of cell death. To examine the effects of copper treatment on the virus, we incubated the copper disks in a viral solution made in PBS, for 5, 10, 20, and 40 min. Afterward, 10 μL of the copper-treated virus solution was introduced to the wells containing the Vero E6 cells. And the infected cells were incubated for 72 h. If these copper disks effectively inactivated the virus, the cell viability after incubating with these copper-treated viruses should be comparable to the uninfected baseline. We found regardless of the type of the copper disks, the cell viabilities increased with the treatment duration (Fig. 3(b)). For the case of treating the virus with the pure copper disk, the cell viability exceeded 100% with 40 min of treatment. And for the cases of viruses treated with CuNW and CuZnNW coated disks, the viability reached 100% with 20 min of treatment. The faster virus inactivation rate of both CuNW and CuZnNW coatings can be attributed to their higher surface area, which is most evident in the 5–10 min time period for CuNW and 10–20 min time period for CuZnNW. In the first 10 min, the virus inactivation rate of CuZnNW coating is similar to that of the pure Cu, and the advantage of the coating's high surface area is seemingly suppressed. This can be attributed to the dual effect of zinc addition. On the one hand, zinc stabilizes the copper ion release and makes the coating effective for a longer time; on the other hand, zinc is oxidized before copper, thus slows the virus inactivation rate until elemental zinc is completely depleted. It should be noted that the electrochemical test is an accelerated process, so the time scale in Fig. 2 and 3 should not be compared directly. Surprisingly, at the 5 min time point, the cell viability of CuNW is less than pure copper and is only slightly
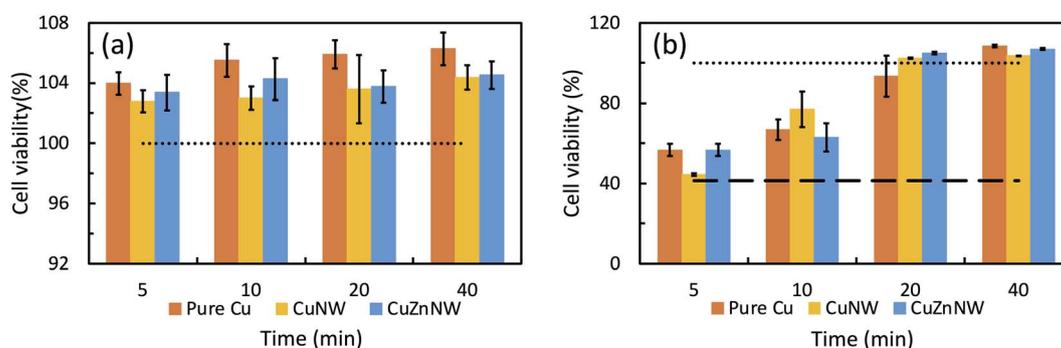

Fig. 3 Viability of Vero E6 cells incubated with (a) phosphate buffer treated by samples and (b) SARS CoV-2 virus–containing phosphate buffer treated by samples. Dotted and dashed lines represent the best and the worst cell viability without copper treatment. The dotted line is the cell viability after incubation without virus, while the dashed line is with the virus.

higher than the dashed line. The exact reason is not yet clear. One possibility is that the surface oxidation layer of CuNW, which is different from that of CuZnNW in the crystal structure, slows down the virucidal effect in the initial stage.

3.5. Thermal gravimetric analysis of HDA and CuNW

In this study, HDA as the capping ligand to stabilize the nanowires, remains in the coating during the virucidal test. HDA is known to absorb virus and disable its infectivity.[18] However, in the nanowire coating, the aliphatic amine has been bonded with the nanowires, making it unavailable for absorbing virus. The binding energy of HDA on Cu is 1.89 eV for Cu(100) and 2.01 eV for Cu(111).[19] The strong HDA–Cu bond does not allow virus to spontaneously replace copper and get absorbed by HDA. After sufficient washing, the excessive HDA is removed from the ink, so the effect of HDA on virus could be neglected, and the virucidal effect of the coating shown in Fig. 3 was dominated by the nanowires themselves. The TGA results of HDA and dried CuNW powders are shown in Fig. 4. The boiling point of the HDA is dependent on its purity and bonding condition. Fig. 4(a) shows that CuNW consists of 13 wt% HAD. The decomposition takes place in a wide temperature range of 125 °C to 500 °C. The non-bonded HDA has a narrower decomposition temperature range of 125 °C to 280 °C without residue. The higher boiling point of nanowire-bonded HDA is due to the extra energy required to break the HDA–Cu bond. Fig. 4(b) shows the decomposition of HDA is a single step event, while the nanowire-bonded HDA has multiple decomposition events beyond 125 °C. We attribute them to the different binding energies of HDA with nanowire and particle (Fig. 1(a) and (d)). Nevertheless, the decomposition peak of CuNW at 125 °C is relatively faint, indicating that majority of free HDA was removed during the washing process.
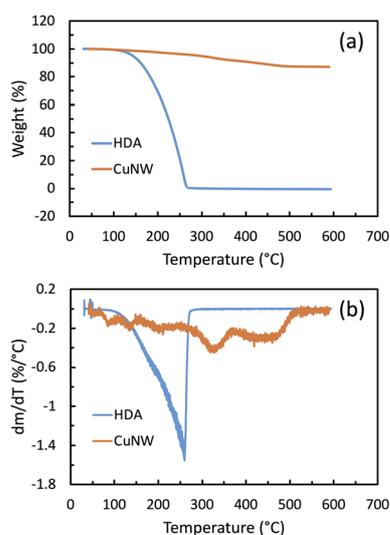
Fig. 4 (a) TGA thermograph of HDA and dried CuNW powder and (b) the derivative of the thermograph. The total mass loss is normalized to 100% when calculating the derivative.
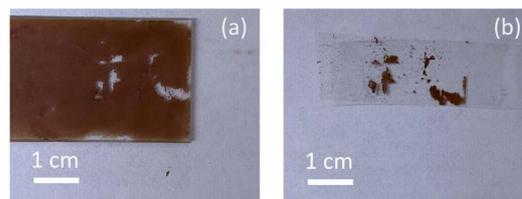
Fig. 5 Cross-cut adhesion measurement of CuZnNW coating on a glass substrate. (a) Before the peel-off test and (b) after the peel-off test.

3.6. Drying and adhesion of the nanowire inks coatings

We have demonstrated that surfaces coated with CuNW and CuZnNW inks can inactivate the SARS CoV-2 virus with a rate comparable to, and in some cases, better than the surface of solid copper. The key advantage of these copper-based nanowire inks is their ease of deployment. They can be sprayed with an airbrush or spray can. The carrying liquid can be water or ethanol. Once applied, the ink dries quickly in about 1 min if ethanol is used. The dried coating adheres to the substrate. The adhesion of our current CuZnNW coating on glass substrates is classified as 2B *via* the cross-cut tape adhesion test, where about 15–35% of the coating area was peeled off. Fig. 5(a) shows the picture of the coating surface after a tape was applied then removed. Fig. 5(b) shows the peeled-off tape with residuals CuZnNW coating. A "2B" adhesion rating is two grades away from the ideal "5B" rating. Possible approaches to improve coating adhesion include substrate surface treatment, blending in acetic acid, changing carrying liquid to polymer-based, or encouraging cold welding of copper nanowires. The coating doesn't need to be thick to be virucidal. Ideally, it should be thin and transparent. When the adhesion issue is fully addressed, the copper-based nanowire ink could be widely used along with other cleaning products on high-touch surfaces as a preventive solution to control the spread of virus.

4. Conclusions

A cost-effective spray-able ink consists of copper–zinc nanowires has been developed. The nanowires contain only a trace amount of zinc, but the coating made of CuZnNW has a noticeable difference to the CuNW coating in the electrochemical properties and virucidal effect. The zinc addition makes the coating more sustainable and effective and it takes only about half of the time to fully deactivate virus in the case of fomite contamination. This CuZnNW ink can be applied to hospital and/or public high-touch surfaces to reduce the risk of virus cross-transmission.

Author contributions

J. Cui conceived and designed the project. C. Pan, K.-S Phadke, and Z. Li performed the synthesis and testing experiments, analysed the data, and wrote the manuscript. G. Ouyang, L. Zhou, and T.-H Kim performed characterization experiments, J. Slaughter raised the funding support for the project and

reviewed the manuscript. B. Bellaire designed the testing method. S. Ren developed the synthesis and coating protocol. All authors discussed the results and commented on the manuscript.

Conflicts of interest

There are no conflicts to declare.

Acknowledgements

References

1 Worldometer, *COVID-19 Coronavirus Pandemic*, https://www.worldometers.info/coronavirus/, accessed, Feburary, 2022.

2 Wits University, *Oxford Covid-19 vaccine trial results*, https://www.wits.ac.za/covid19/covid19-news/latest/oxford-covid-19-vaccine-trial-results.html, accessed, June 2021.

3 Centers for Disease Control and Prevention, *Scientific Brief: SARS-CoV-2 Transmission*, https://www.cdc.gov/coronavirus/2019-ncov/science/science-briefs/sars-cov-2-transmission.html#print, accessed, August 2021.

4 N. Van Doremalen, T. Bushmaker, D. H. Morris, M. G. Holbrook, A. Gamble, B. N. Williamson, A. Tamin, J. L. Harcourt, N. J. Thornburg, S. I. Gerber and J. O. Lloyd-Smith, *N. Engl. J. Med.*, 2020, **382**, 1564.

5 S. Riddell, S. Goldie, A. Hill, D. Eagles and T. W. Drew, *Virology Journal*, 2020, **17**, 1.

6 S. L. Warnes, Z. R. Little and C. W. Keevil, *MBio*, 2015, **6**, e01697.

7 G, C. Grass, Rensing and M. Solioz, *Appl. Environ. Microbiol.*, 2011, **77**, 1541.

8 G. Borkow and J. Gabbay, *Curr. Chem. Biol.*, 2009, **3**, 272.

9 J. Konieczny and Z. Rdzawski, *Arch. Comput. Mater. Sci. Surf. Eng.*, 2012, **56**, 53.

10 C. E. Santo, E. W. Lam, C. G. Elowsky, D. Quaranta, D. W. Domaille, C. J. Chang and G. Grass, *Appl. Environ. Microbiol.*, 2011, **77**, 794.

11 S. L. Warnes and C. W. Keevil, *PloS One*, 2013, **8**, e75017.

12 M. G. Schmidt, H. H. Attaway, S. E. Fairey, J. Howard, D. Mohr and S. Craig, *Appl. Environ. Microbiol.*, 2019, **86**, e01886.

13 A. L. Casey, D. Adams, T. J. Karpanen, P. A. Lambert, B. D. Cookson, P. Nightingale, L. Miruszenko, R. Shillam, P. Christian and T. S. Elliott, *J. Hosp. Infect.*, 2010, **74**, 72.

14 N. Hutasoit, B. Kennedy, S. Hamilton, A. Luttick, R. A. Rashid and S. Palanisamy, *Manuf. Lett.*, 2020, **25**, 93.

15 M. E. Johnson, D. Blankschtein and R. Langer, *J. Pharm. Sci.*, 1997, **86**, 1162.

16 P. L. Honeywell-Nguyen, G. S. Gooris and J. A. Bouwstra, *J. Invest. Dermatol.*, 2004, **123**, 902.

17 S. S. Tinkle, J. M. Antonini, B. A. Rich, J. R. Roberts, R. Salmen, K. DePree and E. J. Adkins, *Environ. Health Perspect.*, 2003, **111**, 1202.

18 H. Noll and J. S. Younger, *Virology*, 1959, **8**, 319.

19 M. J. Kim, S. Alvarez, T. Yan, V. Tadepalli, K. A. Fichthorn and B. J. Wiley, *Chem. Mater.*, 2018, **30**, 2809.